Reversible, Surface-Controlled Structure Transformation in Nanoparticles Induced by an Aggregation State

Feng Huang,* Benjamin Gilbert, Hengzhong Zhang, and Jillian F. Banfield

Department of Earth and Planetary Science, University of California–Berkeley, Berkeley, California 94720-4767, USA

(Received 18 February 2003; published 13 April 2004)

The structure of 3 nm ZnS nanoparticles differs from that of bulk ZnS and is shown to vary with the particle aggregation state. Dispersed or weakly aggregated nanoparticles in suspension have a more distorted internal structure than strongly aggregated nanoparticles. Reversible switching between distorted and crystalline structures can be induced by changing the aggregation state via slow drying and ultrasonic agitation. The transformation was analyzed using pair distribution function data from wide angle x-ray diffraction and the aggregation state monitored via small angle x-ray scattering. Molecular modeling provides insight into particle-particle interactions that induce the structural changes. The reversible nature also implies a low activation energy of nanoparticle transformation and indicates that distorted nanoparticles are not trapped in a metastable state.

DOI: 10.1103/PhysRevLett.92.155501 PACS numbers: 61.46.+w, 64.70.Nd, 65.80.+n, 78.67.Bf

The surface contribution to the total energy becomes increasingly important as the particle size decreases [1–3] and, for very fine particles, may be structure determining. Phase stability crossovers have been experimentally observed when the surface area is very large, due to differences in the surface free energy of polymorphs [4–7]. Factors that directly modify the surface free energy should significantly perturb the total energy of very small particles and could lead to structural transitions without change in particle size.

The surface free energy of nanoparticles in solution can be modified by changes in *p*H or ionic strength [8] and by surface-bound ligands [9,10]. An irreversible room temperature structural transformation has been observed to follow water binding [11]. Here we report that changes in the aggregation state induce reversible internal structural transformations in ZnS nanoparticles suspended in methanol.

Nanoparticles of ZnS were synthesized in anhydrous methanol by mixing Na_2S and $ZnCl_2$ under a N_2 atmosphere. The average size of the as-synthesized nanoparticles is ~3.2 nm, based on high-resolution transmission electron microscope (TEM) observations. Scherrer analysis of x-ray diffraction (XRD) peak broadening suggests a particle size of ~1.2 nm, significantly less than the TEM result. As discussed below, this discrepancy suggests considerable strain in the as-synthesized nanoparticles. The extremely low solubility of ZnS in methanol limits further particle growth.

In Fig. 1(a), we show conventional XRD (Co target) patterns of as-synthesized, aggregated, and redispersed 3 nm ZnS nanoparticles, collected under an x-ray transparent film to limit methanol evaporation. Background contributions from the film and methanol solvent were subtracted from all XRD data from wet samples. The pattern for the as-synthesized nanoparticles exhibits a broad 2-peak pattern [Fig. 1(a), curve *A*].

The aggregation state of nanoparticles can be changed by varying the rate of methanol removal during drying. After slow drying by methanol removal in a 200 Torr atmosphere over 24 h at room temperature, the XRD pattern [Fig. 1(a), curve *B*] exhibits a sharper 3-peak pattern, in which the (220) and (311) reflections from the zinc blende (sphalerite) structure are apparent. When dispersed ZnS nanoparticles in methanol are rapidly dried (4 h in a 10^{-2} Torr atmosphere) then x rayed in methanol immediately, the XRD pattern is essentially identical to that from the as-synthesized material.

0.1 g of the slowly dried ZnS nanoparticles suspended in 4 mL of methanol were redispersed by ultrasonic agitation for 24 h. The corresponding XRD pattern exhibits a broad 2-peak pattern [Fig. 1(a), curve *C*] that closely resembles curve *A*. A further cycle of slow drying and subsequent dispersal in methanol was performed. The XRD patterns of material that was slowly redried (curve *D*) and subsequently resuspended and ultrasonically dispersed (curve *E*) closely resemble curves *B* and *C* (or *A*), respectively. We note that disaggregation of the nanoparticles following the first drying event is not complete, as the line shape of curve *A* in Fig. 1(a) is not completely recovered in curves *C* and *E*.

In a parallel set of experiments [Fig. 1(b)], we further investigated differences in structural state as a function of aggregation state by comparing rapidly to slowly dried powders. All samples were x rayed dry. In Fig. 1, comparison of curves *A* and *A′* show that rapid drying has no significant effect on nanoparticle structure. The rapidly dried sample was resuspended in methanol for 24 h, then dried slowly. The XRD pattern from this sample [Fig. 1(b), curve *B′*] shows three peaks, resembling the pattern in Fig. 1(a), curve *B*. This slowly dried sample was again resuspended in a small amount of methanol and ultrasonically agitated. After 30 min, the methanol was removed, the suspended particles recovered by rapid

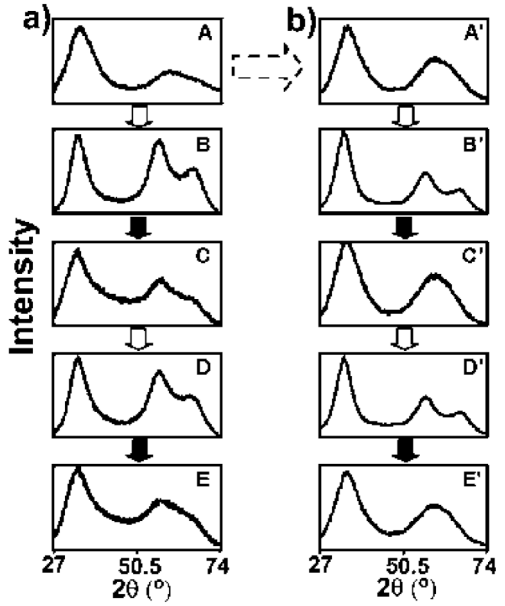

FIG. 1. XRD of ZnS nanoparticles illustrating structure switching due to changes in the aggregation rate. Panel (a) Samples x rayed in methanol showing the sequential steps: (*A*) ZnS nanoparticles synthesized in methanol; (*B*) after slowly drying in a 200 Torr atmosphere; (*C*) after ultrasonic treatment in methanol for 24 h; (*D*) after drying and resuspension in methanol; (*E*) after ultrasonic treatment for 24 h. Panel (b) XRD of ZnS nanoparticles treated similarly to the series in (a), but x rayed dry. (*A'*) ZnS nanoparticles synthesized in methanol, rapidly dried in 10^{-2} Torr; (*B'*) after soaking in methanol for 24 h and slowly drying in a 200 Torr atmosphere; (*C'*) after ultrasonic treatment in methanol (see text for details) and rapid drying in 10^{-2} Torr; (*D'*) after reemersion in methanol for 24 h and slow drying in a 200 Torr atmosphere; (*E'*) after further ultrasonic dispersal in methanol and rapid drying in 10^{-2} Torr.

drying, and the sample stored in argon to prevent hydration. A small amount of methanol was added to the as yet undispersed particles, which were then ultrasonically agitated for another 30 min. The suspended particles were again recovered by rapid drying. This procedure was repeated until sufficient rapidly dried sample was recovered for x-ray diffraction analysis and further experiments.

The XRD pattern of redispersed nanoparticles that were dried rapidly closely resembles the initial as-synthesized pattern [Fig. 1(b), curve *C'*]. The rapidly dried sample was then resuspended and slowly dried, as described above. The XRD pattern typical of slowly aggregated material [Fig. 1(b), curve *B'*] was recovered [Fig. 1(b), curve *D'*]. Subsequently, the material was redispersed in methanol and rapidly dried, as described above. The XRD pattern [Fig. 1(b), curve *E'*] is indistinguishable from Fig. 1(b), curve *C'* and from the initial material.

It was possible to cycle perfectly between structural states when the sample was x rayed dry [Fig. 1(b)] but the cycling was imperfect when samples were x rayed in methanol [Fig. 1(a)]. This was attributed to partial reaggregation of nanoparticles in methanol during the XRD experiment. To verify this, we allowed the rapidly dried sample [Fig. 1(a), curve *C*] to sit in methanol for 3 d without ultrasonic agitation. The XRD pattern (not shown) was closely similar to that shown in Fig. 1(a), curve *B*. In contrast, the XRD pattern of rapidly dried nanoparticles was stable over 20 d if the sample was stored in an anhydrous atmosphere.

To further characterize the structures of dispersed and of aggregated ZnS nanoparticles, we performed synchrotron wide-angle x-ray scattering (WAXS) of the samples used to collect data in Fig. 1(b). We acquired WAXS data to high values of diffraction vector, Q, and generated the real-space pair distribution function (PDF) by standard methods [12,13]. To characterize the aggregation state of dispersed and slowly dried material, we additionally performed small-angle x-ray scattering (SAXS) of the same samples. SAXS is widely used for nanoparticle size analysis, can determine the fractal dimension of aggregates, and has been used to study interparticle interactions [14–16].

Figure 2 shows the WAXS (3a), PDF (3b), and SAXS (3c) patterns of the ZnS sample in the state corresponding to A'-E' in Fig. 1(b). The WAXS and PDF patterns of C' (or E') and D' reproduce A' and B', respectively, very well across large ranges in Q and R, where R is the real-space interatomic distance.

The slowly dried nanoparticles give sharper peaks in both XRD and WAXS patterns, and show longer-range correlations in the PDF. This behavior is reversible, and hence cannot be attributed to growth of the nanoparticles. The WAXS and PDF patterns of rapidly and slowly dried nanoparticles possess differences not consistent with either size changes or Debye-Waller disorder alone or in combination. Interatomic correlation peaks in the PDF patterns differ in both position and width. The only reasonable interpretation is that the as-synthesized and rapidly aggregated nanoparticles contain considerable distortion. The disorder present in as-synthesized ZnS nanoparticles explains the discrepancy between size determination from TEM and from Scherrer analysis of x-ray diffraction peak broadening.

The SAXS patterns show that changes in degree of structural distortion within nanoparticles correlate with changes in the aggregation state, which can be reversibly modified by slow drying and resuspension. In Fig. 3(c), the linear trends in the low-Q region ($Q < 0.03$ Å^{-1}) indicate that both rapidly dried and slowly dried 3 nm ZnS nanoparticles form long-range aggregates that obey fractal geometry. In fractal objects, the mass within a sphere of radius r is proportion to r^D, where D is the fractal dimension [16]. The SAXS data indicate that the fractal dimension is different for nanoparticle aggregates that have been rapidly or slowly dried. For rapidly dried aggregates $D = 2.6 \pm 0.1$, while for slowly dried aggregates $D = 2.9 \pm 0.1$.

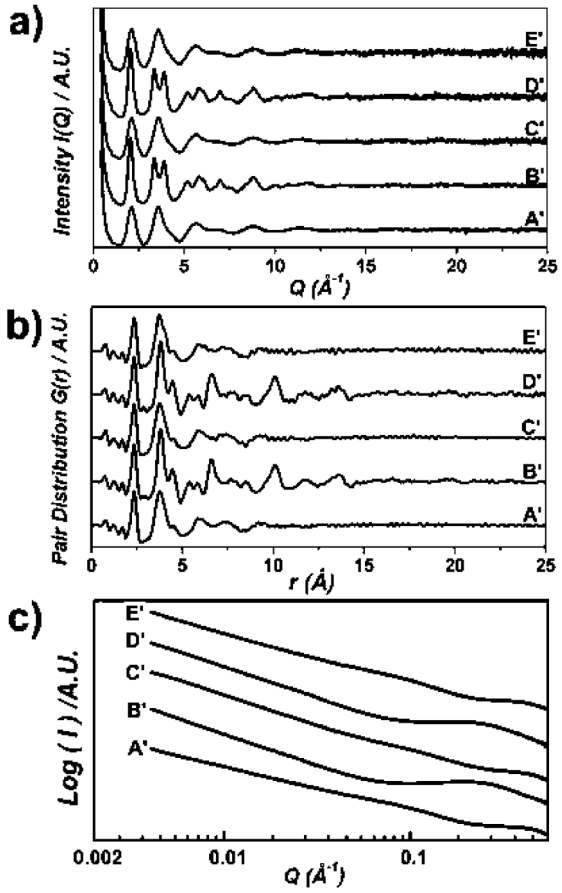

FIG. 2. (a) Wide angle x-ray scattering (WAXS), (b) pair distribution function (PDF), and (c) small angle x-ray scattering (WAXS) pattern of ZnS nanoparticles in aggregation states A' to E' in Fig. 1(b).

The SAXS data also show significant differences in the high-Q region. The data in this region probe length scales comparable to the nanoparticle diameter, and are difficult to interpret for the high concentration aggregates studied here. An analytical expression for the scattering function is not available, and simple data treatments, such as Guinier analysis, are unreliable in this regime. However, we can conclude that the interparticle correlations over short distances change reversibly throughout the treatment cycle. The fractal dimension analysis strongly suggests that the nanoparticle packing efficiency in the aggregates is higher following slow drying.

We propose that the interparticle surface interactions that accompany nanoparticle aggregation cause the structural changes detected in the x-ray diffraction experiments. The observation of oriented aggregation-based crystal growth in ZnS [17] and TiO_2 [18] nanoparticles confirm that very short-range particle-particle interactions occur in solution. Both Coulombic and very short-range non-Coulombic interactions between surface atoms of different particles allow the reduction of surface tension (i.e., strain). We conclude that structural transformation upon aggregation requires a critical number of particle-particle interactions. Consequently, the aggregation kinetics are critical in determining the structural state of uncoated ZnS nanoparticles.

The observation of reversible structure switching between nanoparticles in different aggregation states indicates that the ZnS nanoparticles are not trapped in a metastable state. As the nanoparticles respond structurally to changes in their surface environments at room temperature we infer that the energy of aggregation and the barriers to transformation are low.

Molecular dynamics (MD) simulations were used to study the effects of interparticle contacts following aggregation [19]. We used interatomic potentials for ZnS developed by Wright and Jackson [20], that have been previously shown to give accurate structures for bulk ZnS and ZnS nanoparticles [10,21]. We first obtained the energy-minimized structure of a 3 nm ZnS nanoparticle and calculated the associated WAXS pattern using the Debye equation. Despite the neglect of weak methanol—ZnS interactions, a good match between the predicted and observed WAXS patterns was obtained [Fig. 3(a)]. The calculated WAXS pattern for a 3 nm nanoparticle cut from undistorted sphalerite [also shown in Figs. 3(a) and 3(b)] is not a good match to the experimental patterns for any sample.

To consider an aggregate, we obtained the energy-minimized structures of five isolated 3 nm ZnS nanoparticles. These nanoparticles were subsequently placed in a single cell, and a further simulation was run. We restrict our analysis to the first period of the simulation, during which the nanoparticles aggregated without coalescence. A view of the structure of one of the aggregated nanoparticles, and the associated WAXS pattern is given in Fig. 3(b). Figure 3(b) shows that the interparticle interactions cause an increase in internal periodicity, in good agreement with experiment. As shown in Fig. 3(c), the aggregated nanoparticles remained well defined, in random orientations, with incomplete bonding at the interfaces.

We estimated the enthalpy of particle aggregation to be $\sim$4 kJ/mol from the difference in molar ZnS total energies in the single particle and aggregated nanoparticle MD simulations [22]. The value is very small compared to the binding energy of Zn or S in ZnS, or to the enthalpy of water binding [10]. Consequently, the MD simulations confirm that the structural transformations result from low energy interparticle interactions. Such low energy interactions are easily reversed (by mechanical agitation), with a corresponding reversal of the structural transformation.

In conclusion, the structure of 3 nm ZnS nanoparticles differs from that characteristic of bulk material, and the difference increases with decrease in nanoparticle packing density. We find that, under appropriate conditions, aggregation-disaggregation causes profound, rapid, reversible structural changes. The as-synthesized and rapidly aggregated ZnS nanoparticles have a distorted

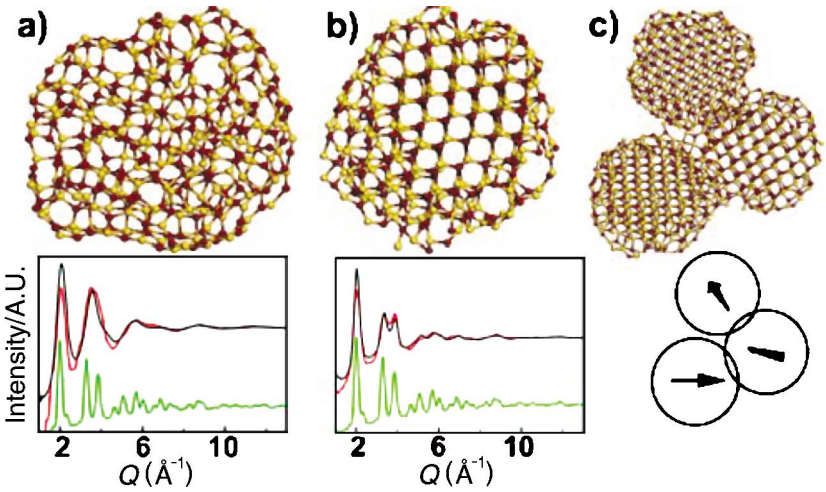

FIG. 3 (color). Molecular dynamics predictions of the structures of (a) an isolated and (b) an aggregated individual 3 nm ZnS nanoparticle, and the calculated WAXS patterns. The nanoparticles are shown in cross section to reveal internal structure. Isolated nanoparticles are distorted and give broad peaks in the calculated WAXS pattern (red line) in agreement with experimental curve A' (black line). Aggregated nanoparticles possess more ordered structures, which produce sharper peaks in the WAXS pattern (red line) in agreement with experimental curve B' (black line). The calculated WAXS pattern of a 3 nm undistorted sphalerite nanoparticle is also shown (green line). (c) A cross section through part of the aggregated MD cluster. The sphalerite 111 directions of each nanoparticle are shown beneath, indicating that the particles have aggregated without coalescence and coarsening.

structure that reflects the minimum energy state, not because they are trapped in a metastable state. In fact, all of the nanoparticles are able to respond to changes in their surface environments at room temperature. Thus, we infer the activation energies for the transformations, and the aggregation energy, are small.

We thank Paul Alivisatos for access to equipment and Glenn Waychunas for helpful discussions. Thanks are extended to Dr. W. Smith, Dr. T. R. Forester, and Dr. D. Fincham for providing MD codes. WAXS and SAXS data were acquired on BESSRC-CAT beam lines 11-ID-C and 12-ID-C at the Advanced Photon Source (APS), and we thank Yang Ren and Soenke Seifert. Financial support for this work came from the U.S. Department of Energy (DE-FG03-01ER15218 and LBNL LDRD 36615) and the National Science Foundation (EAR-0123967). Use of the Advanced Photon Source was supported by the U.S. Department of Energy, Office of Science, Office of Basic Energy Sciences, under Contract No. W-31-109-Eng-38.

*Corresponding author.
Email address: fhuang@eps.berkeley.edu
Current address: Fujian Institute of Research on the Structure of Matter, Chinese Academy of Sciences, Fuzhou, Fujian, 350002, China.

[1] J. A. Nuth, Nature (London) **329**, 589 (1987).
[2] M. Y. Gamarnik, Nanostruct. Mater. **7**, 651 (1996).
[3] R. C. Garvie, J. Phys. Chem. **82**, 218 (1978).
[4] J. M. McHale *et al.*, Science **277**, 788 (1997).
[5] H. Z. Zhang *et al.*, J. Mater. Chem. **8**, 2073 (1998).
[6] A. Navrotsky, Geochim. Cosmochim. Acta **66**, A548 (2002), Suppl. 1.
[7] M. Ranade *et al.*, Abstr. Pap. Am. Chem. Soc., **223**, 148-Geoc Pt. 1 (2002).
[8] L. Vayssieres *et al.*, Pure Appl. Chem. **72**, 47 (2000).
[9] K. Murakoshi *et al.*, Chem. Commun. **3**, 321 (1998).
[10] M. Haase *et al.*, J. Phys. Chem. **96**, 6756 (1992).
[11] H. Zhang *et al.*, Nature (London) **424**, 1025 (2003).
[12] B. J. Thijsse, J. Appl. Crystallogr. **17**, 61 (1984).
[13] J. Urquidi *et al.*, J. Appl. Crystallogr. **36**, 368 (2003).
[14] F. Meneau *et al.*, Faraday Discuss. **122**, 203 (2003).
[15] H. Mattoussi *et al.*, Phys. Rev. B **58**, 7850 (1998).
[16] J. Teixeira, J. Appl. Crystallogr. **21**, 781 (1988).
[17] F. Huang *et al.*, Nano Lett. **3**, 373 (2003).
[18] R. L. Penn *et al.*, Science **281**, 969 (1998).
[19] In the MD simulation, the covalent compound ZnS was described using a shell model [20]. Simulations were done in a canonical ensemble at 300 K using the Nose-Hoover algorithm with a time step of 0.5 fs. Simulations were calculated under vacuum conditions, neglecting the methanol solvent. This approximation was considered acceptable for qualitative analysis because methanol is not expected to strongly interact with the ZnS surface. The MD initial configurations were as follows: for an isolated nanoparticle, a 3 nm spherical zinc blende particle cut from the coordinates of the bulk structure; for the aggregation simulation, a cluster of five similar nanoparticles arranged in a tetrahedral geometry (randomly oriented, one at the center and in each of the corners). Both systems reached a steady energy state after similar simulation time (15–40 ps).
[20] K. Wright *et al.*, J. Mater. Chem. **5**, 2037 (1995).
[21] H. Zhang *et al.*, J. Phys. Chem. B **107**, 13 051 (2003).
[22] Neglect of the methanol solvent will lead to an overestimation of the enthalpy of aggregation, as methanol binding energy is neglected. The errors associated by the neglect of methanol are small relative to all other sources of error.